JOURNAL OF GUIDANCE, CONTROL, AND DYNAMICS
Vol. 24, No. 3, May–June 2001

Neoclassical Guidance for Homing Missiles

Pini Gurfil*
Princeton University, Princeton, New Jersey 08544
Mario Jodorkovsky†
RAFAEL, Ministry of Defense, 31021 Haifa, Israel
and
Moshe Guelman‡
Technion—Israel Institute of Technology, 32000 Haifa, Israel

A new approach to guidance of homing missiles is considered. Like classical proportional navigation (PN), the new guidance law utilizes line-of-sight (LOS) rate measurement only. However, its performance is superior to PN, in the sense that zero-miss-distance (ZMD) is obtained against highly maneuvering targets. This merit is achieved with neither the estimation of target maneuver nor time to go. In the derivation of the new guidance law, a linearized formulation of the PN interception kinemtics is used. Based on the method of adjoints, it is proved analytically that when the overall transfer function of the missile is biproper, that is, the degree of the numerator equals the degree of the denominator, ZMD is obtained. The ZMD property holds in the following cases: deterministic target maneuvers, random target maneuvers, deterministic target maneuvers with random starting times, fading noise, and passive- and active-receiver noise. The realization of the new guidance law requires lead compensation. When LOS rate measurement is corrupted by noise, lead–lag compensation can be used instead. These design considerations are illustrated in simulations, which verify that negligible miss distance against highly maneuvering targets is obtained even when the LOS rate measurement is noisy.

Nomenclature

a	=	lateral acceleration
N'	=	effective proportional navigation constant
R	=	missile-target relative range
r	=	relative order of a rational function
t_f	=	flight time
V	=	velocity
V_C	=	closing velocity
y	=	missile-target relative vertical position
$y(t_f)$	=	miss distance
γ	=	flight-path angle
ζ	=	damping coefficient
λ	=	line-of-sight angle
τ	=	time to go
τ_1	=	missile time constant
ω_n	=	natural frequency

Subscripts

C	=	commanded value
f	=	final value
M	=	missile
T	=	target
0	=	initial value

I. Introduction

THE challenging problem of missile guidance has been treated using several basic methodologies. The classical approach is to apply missile maneuver acceleration proportionally to the measured line-of-sight (LOS) rate. The resulting guidance law is the well-known proportional navigation (PN). The modern approach to missile guidance is based on optimal control theory (one-sided optimization) and differential games (two-sided optimization).

PN is probably the method most commonly used for guidance of homing missiles, and a vast amount of literature exists on the subject (e.g., see Refs. 1 and 2 and the references therein). Modern guidance laws have also been thoroughly analyzed.[3–5] PN is known to yield reasonable miss distance when applied against nonmaneuvering or moderately maneuvering targets, whereas modern guidance laws can theoretically achieve zero-miss distance (ZMD) against highly maneuvering targets. This merit is obtained at the expense of additional information, required for the implementation of these guidance laws. In particular, an estimation of time to go and target maneuver is required. The latter requirement is not a simple task to follow, and even when fulfilled, due to the inherent time delay of the estimator,[6–8] the guidance law performance deteriorates. Also, modern guidance laws are often quite complicated; closed-form solutions exist only when system dynamics are neglected or approximated to first-order[9] or second-order[10] transfer functions. This complexity demands a considerable real-time computational capability. Furthermore, because modern guidance laws result in an inverse of the system dynamics, their robustness has been doubted.[11]

In this paper, we suggest an alternative approach to missile guidance. The guidance law conceived relies on LOS rate measurement only, like the classical PN, yet its performance is similar to modern guidance laws, in the sense that ZMD can be obtained against highly maneuvering targets. This approach is therefore called the neoclassical approach to missile guidance. Consequently, the main purpose of the paper is to present a new guidance law based on LOS rate measurement only, the main features of which are as follows:

1) In the case where LOS rate measurement is not corrupted by noise, the new guidance law yields ZMD for any flight time, against targets performing an arbitrary (bounded) deterministic maneuver, random maneuver, or deterministic maneuver with a random starting time.

2) The new guidance law yields ZMD for all flight times in the case of stochastic inputs, such as fading noise and passive- and active-receiver noise.

3) In the case where the LOS rate measurement is corrupted by noise, a straightforward modification will give near-ZMD performance.

Received 14 January 2000; revision received 9 August 2000; accepted for publication 30 August 2000.

*Research Associate, Mechanical and Aerospace Engineering Department; pgurfil@princeton.edu. Member AIAA.

†Senior Research Scientist, P.O. Box 2250, Department 39; marioj@rafael.co.il.

‡Professor and Head, Asher Space Research Institute, Faculty of Aerospace Engineering; aerglmn@aerodyne.technion.ac.il.

4) The maneuver acceleration required to achieve ZMD performance remains within reasonable limits, such that the overall maneuver effort is smaller than that required by PN guidance (PNG).

In the derivation of our neoclassical guidance law, called ZMD–PNG, we rely on the basic kinematic scenario used for the formulation of the PNG interception problem. Although in the general case PNG is a nonlinear control problem, to apply known techniques of analysis and design, the system equations are linearized, yielding an equivalent linear time-varying system. The linearization is valid when it is assumed that the missile and target approach the so-called collision course. It is known that the linearized model faithfully represents the guidance dynamics[2,12,13] and that the miss distance associated with the linear approximation is very close to that obtained from the nonlinear mode.[2,13]

A most popular tool for the analysis of the linear PNG loop is the method of adjoints.[2,14,15] This technique is based on the adjoint system impulse response and can be used to analyze miss distance caused by arbitrary inputs to the PNG system. Although this method renders analytical expressions for the miss distance as a function of flight time, it is very difficult to get closed-form solutions for high-order systems or for cases where the effective PN constant is not an integer. Thus, the use of this method is mainly numerical, that is, simulations of the adjoint loop are carried out to analyze miss distance. Except for simple cases,[2,15] no direct design information is available.

In this paper, the adjoint formulas are utilized to the derivation of the ZMD–PNG law. We first examine the miss-distance formulas for three main cases: deterministic target maneuvers, stochastic inputs (such as fading noise, passive- and active-receiver noise, and random target maneuver) and deterministic target maneuvers with random starting times. The key observation is that when the dynamics of the guidance loop, given by some transfer function, is biproper, that is, the degree of the numerator equals the degree of the denominator, ZMD is rendered for all cases mentioned. This, of course, requires lead compensation, which can be achieved by augmenting the guidance commands by proportional-derivative controller. However, lead compensation causes noise amplification problems when the LOS rate measurement is corrupted by noise. However, one can use lead–lag compensation instead, such that near-ZMD is obtained. These design considerations are illustrated in simulations, which verify that ZMD–PNG gives negligible miss distance against highly maneuvering targets, even when the LOS rate measurement is noisy.

An additional contribution of this paper is that it connects between the PNG loop so-called finite time stability and miss distance. It was conjectured,[13,16,17] based on empirical experience, that a strong relationship exists between finite time stability and miss distance. By defining the concept of finite time global absolute asymptotic stability (FT-GAAS) and the utilization of the circle criterion, we show that if the system is FT-GAAS until the end of the flight there will be no miss distance.

The paper is organized as follows. Section II presents the mathematical modeling of the linearized PNG loop and formulates the problem of ZMD–PNG. Section III outlines the class of transfer functions that yield ZMD and stresses some design implications. In Sec. IV, illustrative examples based on numerical simulations are presented. We conclude our discussion in Sec. V.

II. Problem Formulation

The general formulation of a three-dimensional PN interception problem is rather complicated. However, assuming that the lateral and longitudinal maneuver planes are decoupled by means of roll control, one can deal with the equivalent two-dimensional problem in quite a realistic manner. We shall further assume that the geometry is two dimensional. In addition to this basic assumption, we shall also assume that the gravitational component of the total missile lateral acceleration is negligible. These assumptions enable the formulation of a general planar interception missile-target geometry as shown in Fig. 1. Figure 1 describes a missile employing PN to intercept a maneuvering target.

Based on Fig. 1, a linearized model of the guidance dynamics can be developed. Such a model is widely used in the analysis of

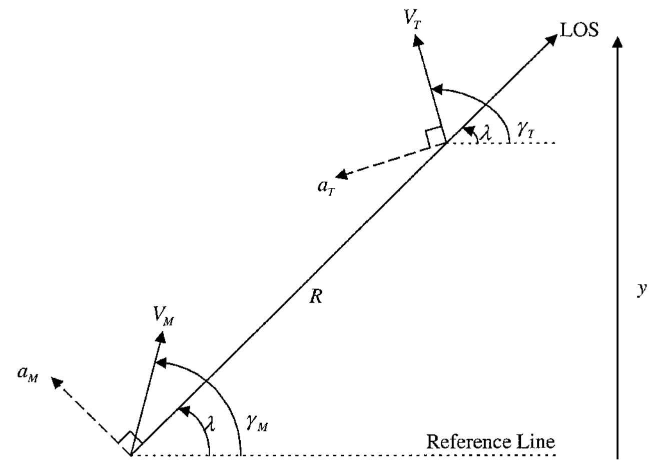

Fig. 1 Interception geometry.

PNG.[1,2,14,18] A block diagram describing the linear model is given in Fig. 2. In this linear time-varying system, missile acceleration a_M is subtracted form target acceleration a_T to form a relative acceleration $\ddot{y}$. A double integration yields the relative vertical position y (see Fig. 1), which at the end of the engagement is the miss distance $y(t_f)$. When the closing velocity V_C is assumed to be constant, the relative range is given by

$$R = V_C \cdot \tau \tag{1}$$

where τ is the time to go, defined as

$$\tau \triangleq t_f - t \tag{2}$$

Dividing the relative vertical position y by the range given in Eq. (1) yields the geometric LOS angle λ. The missile seeker is represented in Fig. 2 as an ideal differentiator with an additional transfer function $G_1(s)$, which represents the LOS rate measurement and noise filtering dynamics. The seeker generates an LOS rate command $\dot{\lambda}_C$, which is multiplied by the PN gain $N' \cdot V_C$ to form a commanded missile maneuver acceleration a_C, with N' being the effective PN constant. The flight control system, whose dynamics are represented by the transfer function $G_2(s)$, attempts to maneuver the missile adequately to follow the desired acceleration command.

A common use of the model shown in Fig. 2 is miss-distance analysis. In particular, the method of adjoints is utilized.[1,2,14,15] The adjoints technique is based on the system impulse response and can be used to analyze miss distance as a function of flight time, provided that the system is linear. This method is utilized to the analysis of miss distance due to deterministic disturbances,[2] stochastic inputs,[14] and deterministic target maneuvers with random starting times.[15] These cases are dealt with hereby. The purpose of the subsequent discussion is to prove that there exists a class of PNG-based systems that yield ZMD for any type of input (deterministic, stochastic, random) and any given flight time.

A. Deterministic Disturbances

In the deterministic case, the miss distance is given by

$$y(t_f) = \mathcal{L}^{-1}\{Q(s) \cdot y_T(s)\} \tag{3}$$

where

$$Q(s) \triangleq \exp\left(N' \int_{\infty}^{s} H(\sigma)\,\mathrm{d}\sigma\right) \tag{4}$$

$$G(s) \triangleq G_1(s)G_2(s) \tag{5}$$

$$H(s) \triangleq G(s)/s \tag{6}$$

$$y_T(s) = \mathcal{L}\{y_T(t)\} \tag{7}$$

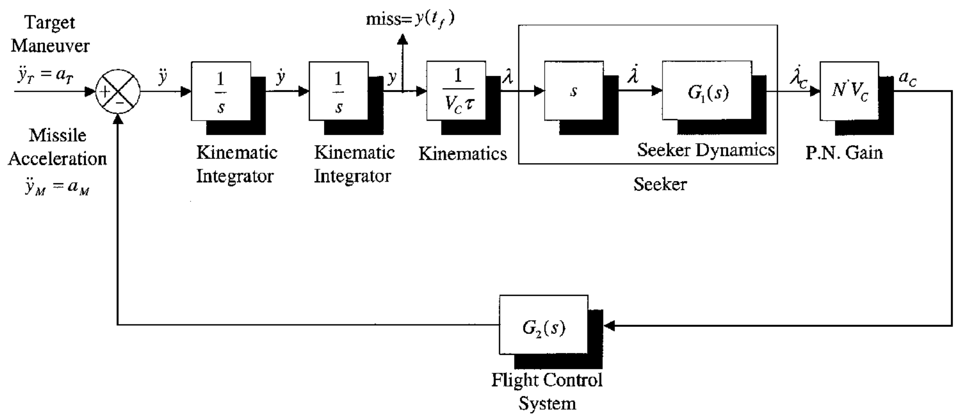

Fig. 2 Linearized PNG model block diagram.

In these expressions, $\mathcal{L}$ is the Laplace transform and $y_T(t)$ the deterministic system input, which can either be an initial condition or a deterministic target maneuver (Fig. 2). $G(s)$ is the LOS rate measurement and flight control dynamics of the PNG loop (see Fig. 2) and is assumed to be asymptotically stable with $G(0) = 1$.

B. Stochastic Inputs

Stochastic inputs are divided into two subcategories: 1) noise inputs, such as fading noise, passive- and active-receiver noise (mainly in radar-guided missiles) and glint noise (mainly in radar-guided missiles and to a much smaller extent, in electro-optical missiles as well) and 2) random target maneuvers, such as the random telegraph maneuver.[14,19]

The expressions for the rms miss distance in these cases, with $Q(s)$ as in Eq. (4), are well known.[2,5]

Here rms miss due to fading noise, which is a range-independent LOS angular noise, is given by

$$\frac{E\left[y^2(t_f)\right]\big|_{\text{fading}}}{\Phi_{\text{fn}}} = \int_0^{t_f} \left\{\mathcal{L}^{-1}\left[\frac{\mathrm{d}Q(s)}{\mathrm{d}s}\right]\right\}^2 \mathrm{d}t \tag{8}$$

where Φ_{fn} is the power spectral density (PSD) of the fading noise, in square radian per hertz.

The rms miss due to passive-receiver noise is

$$\frac{E\left[y^2(t_f)\right]\big|_{\text{passive}}}{\Phi_{\text{pn}}} = \int_0^{t_f} \left\{\mathcal{L}^{-1}\left[\frac{\mathrm{d}^2Q(s)}{\mathrm{d}s^2}\right]\right\}^2 \mathrm{d}t \tag{9}$$

where Φ_{pn} is the PSD of the passive-receiver noise, in square radian per hertz.

The rms miss due to active-receiver noise is

$$\frac{E\left[y^2(t_f)\right]\big|_{\text{active}}}{\Phi_{\text{an}}} = \int_0^{t_f} \left\{\mathcal{L}^{-1}\left[\frac{\mathrm{d}^3Q(s)}{\mathrm{d}s^3}\right]\right\}^2 \mathrm{d}t \tag{10}$$

where Φ_{an} is the PSD of the active-receiver noise, in square radian per hertz.

The rms miss due to glint noise is

$$\frac{E\left[y^2(t_f)\right]\big|_{\text{glint}}}{\Phi_{\text{gn}}} = \int_0^{t_f} \{\mathcal{L}^{-1}[1 - Q(s)]\}^2 \,\mathrm{d}t \tag{11}$$

where Φ_{gn} is the PSD of the glint noise, in square radian per hertz.

A well-known example for a random target maneuver is the random telegraph. A random telegraph maneuver represents a policy, starting at time zero, in which the target executes either a maximum positive or negative acceleration $\pm a_T$ such that the number of sign changes per second follows a Poisson distribution and the average number of sign changes is ν per second. By the demand of equivalence of second-order miss distance statistics, the random sequence can be represented as a white noise passing through a shaping filter.[20] Thus, the following expression for the rms miss distance is obtained[14,20]:

$$\frac{E\left[y^2(t_f)\right]\big|_{\text{RT}}}{\Phi_{\text{RT}}} = \int_0^{t_f} \left\{\mathcal{L}^{-1}\left[\frac{1}{s/(2\nu)+1}\cdot\frac{Q(s)}{s^2}\right]\right\}^2 \mathrm{d}t \tag{12}$$

where $\Phi_{\text{RT}} = (a_T)^2_{\max}/\nu$ is the PSD of the white noise, passing through the shaping filter $P(s) = 1/[s/(2\nu) + 1]$.

C. Deterministic Target Maneuvers with Random Starting Times

The target might initiate a maneuver at some random time during flight. It is assumed that the probability distribution function of the maneuver starting time is known. For instance, assume that the target performs a constant maneuver a_T whose starting time is uniformly distributed over the flight time. By the demand of equivalence of second-order miss distance statistics, this maneuver can be described as a white noise, with PSD $\Phi_S = a_T^2/t_f$ passing through the shaping filter $1/s$ (Ref. 2). In this case, the rms miss distance is given by

$$\frac{E\left[y^2(t_f)\right]\big|_S}{\Phi_S} = \int_0^{t_f} \left\{\mathcal{L}^{-1}\left[\frac{Q(s)}{s^3}\right]\right\}^2 \mathrm{d}t \tag{13}$$

Another possibility is that the target performs a sinusoidal maneuver, whose starting time is uniformly distributed, that is, the phase of the maneuver, φ, is a random variable:

$$a_T(t) = a_T \sin(\omega_T t + \varphi) \tag{14}$$

The random-phase sinusoidal maneuver can be represented as a white noise with PSD $\Phi_{\sin} = a_T^2/t_f$ passing through the shaping filter $P(s) = 1/\lfloor \omega_T(s/\omega_T)^2 + \omega_T \rfloor$. The rms miss distance is given by[14]

$$\frac{E\left[y^2(t_f)\right]\big|_{\sin}}{\Phi_{\sin}} = \int_0^{t_f} \left\{\mathcal{L}^{-1}\left[\frac{1/\omega_T}{(s/\omega_T)^2+1}\cdot\frac{Q(s)}{s^2}\right]\right\}^2 \mathrm{d}t \tag{15}$$

In the general case, any target maneuver with random starting time can be represented as a white noise with PSD Φ_{in} passing through a shaping filter $P(s)$. Thus, the rms miss distance is given by[14]

$$\frac{E\left[y^2(t_f)\right]}{\Phi_{\text{in}}} = \int_0^{t_f} \left\{\mathcal{L}^{-1}\left[P(s)\cdot\frac{Q(s)}{s^2}\right]\right\}^2 \mathrm{d}t \tag{16}$$

In the subsequent discussion, we shall address the following problem: Determine the set of all possible strictly proper transfer functions $H(s)$, defined in Eq. (6), such that the miss distance becomes zero for all flight times and all possible deterministic, stochastic, and random inputs to the guidance systems. That is, we wish to find the following class:

$$\boldsymbol{H} = \{H(s) : y(t_f) \equiv 0 \quad \forall t_f\} \tag{17}$$

Notice that due to the definition of $H(S)$ given in Eq. (6) finding the class $\boldsymbol{H}$ immediately characterizes the set $\boldsymbol{G}$, where

$$\boldsymbol{G} = \{G(s) : y(t_f) \equiv 0 \quad \forall t_f\} \tag{18}$$

III. Class of All PNG-Based Systems Yielding ZMD

Exclude for the moment the miss distance due to glint [Eq. (11)]. Notice that in all other cases [Eqs. (3), (8–16)], if $Q(s)$ had been identically equal to zero, no miss distance would have been obtained. Thus, to characterize the class of ZMD PNG-based systems, we have to find when $Q(s)$ equals zero. To begin, we notice that Eq. (4) can be rewritten into the following form:

$$Q(s) = e^{N'F(s)} \big/ e^{N'F(\infty)} \tag{19}$$

where

$$F(x) \triangleq \left[\int H(\sigma)\, \mathrm{d}\sigma \right]_{\sigma = x} \tag{20}$$

Since $e^{N'F(s)} \not\equiv 0$, $Q(s) \to 0$ if and only if $e^{N'F(\infty)} \to \infty$, which requires $F(\infty) \to \infty$. Hence, it is required to determine $H(s)$ for which $F(\infty) \to \infty$. To do this, the following theorem is introduced.

Theorem: Consider a strictly proper rational function of the form

$$H(s) = \frac{b(s)}{a(s)} = \frac{b_1 s^{n-1} + b_2 s^{n-2} + \cdots + b_n}{s^n + a_1 s^{n-1} + \cdots + a_n}, \qquad b_1 \geq 0 \tag{21}$$

where $a(s)$, $b(s)$ are coprime polynomials.

Denote by r the relative order of $H(s)$, that is, $r \triangleq \deg[a(s)] - \deg[b(s)]$. Under these conditions,

$$F(\infty) = \lim_{\sigma \to \infty} \left[\int H(\sigma)\, \mathrm{d}\sigma \right] \to \begin{cases} 0 & \text{iff} \quad r \geq 2 \\ \infty & \text{iff} \quad r = 1 \end{cases} \tag{22}$$

Proof: See Appendix A. □

The relevance of the theorem to the classification of all PNG-based systems rendering ZMD is clarified by means of the following corollary.

Corollary of Theorem: $G(s) \in \boldsymbol{G}$ if and only if $b_1 > 0$, that is, $G(s)$ is biproper (i.e., the degree of the numerator equals the degree of the denominator),

$$\boldsymbol{G} = \{G(s) : b_1 > 0\} \tag{23}$$

Proof: In the theorem, take $H(s) = G(s)/s$. According to this theorem, $F(\infty) \to \infty$ if and only if $r[H(s)] = 1$. Thus, since $r[H(s)] = r[G(s)/s] = r[G(s)] + r[s] = 1$, $r[G(s)] = 0$, which means that $G(s)$ is biproper. □

The set $\boldsymbol{G}$ contains all of the transfer function $G(s)$ that impose ZMD to the PNG system shown in Fig. 2. Note that the theorem 1 and its corollary provide necessary and sufficient conditions. Consequently, if $y(t_f) \equiv 0 \;\; \forall t_f$, then $G(s) \in \boldsymbol{G}$; and conversely, if $G(s) \in \boldsymbol{G}$, then $y(t_f) \equiv 0 \;\; \forall t_f$.

The interpretation of the theorem and its corollary should be as follows. If $G(s)$, the dynamics of the PNG loop, is biproper, that is, the degree of the numerator equals the degree of the denominator, the miss distance will be identically zero for all flight times and all deterministic or random target maneuvers. Furthermore, in the stochastic case, ZMD is obtained for the cases of fading and passive- and active-receiver noise inputs. Because in general $G(s)$ is a strictly proper transfer function, that is, the degree of the denominator is greater than the degree of the numerator, a guidance controller comprised of lead networks, such as proportional–derivative (PD) controllers, should be added. However, pure lead causes noise amplification problems. Thus, instead of pure lead compensation, lead–lag networks should be used. In this case, the miss distance is not identically zero, but it is reduced dramatically, as shown in the simulations described in Sec. IV. The PN-based guidance law with the appropriate compensation will be called hereafter ZMD–PNG.

Note that the case of glint noise is different from all other inputs. Observe that in the stochastic case the expressions for miss distance comprise derivatives of $Q(s)$, whereas in the case of glint [Eq. (11)], the miss distance is calculated by taking the inverse Laplace transform of $1 - Q(s)$. Consequently, we notice that if $Q(S) \equiv 0$, then for long flight times

$$\frac{E\left[y^2(t_f)\right]\big|_{\text{glint}}}{\Phi_{\text{gn}}} = \int_0^\infty \mathcal{L}^{-1}(1)\, \mathrm{d}t = \int_0^\infty \delta(t)\, \mathrm{d}t = 1 \tag{24}$$

That is, the rms miss distance due to glint will be from the order of magnitude of the PSD of the noise. This implies that the implementation of the ZMD–PNG law is more appropriate in low glint systems, such as missiles with electro-optical seekers, rather than in missiles with radar seekers, where the glint is much more dominant.

As mentioned, ZMD can be obtained by employing modern guidance as well. However, perhaps the most important advantage of the ZMD-PNG over modern guidance laws is that it requires neither the estimation of target maneuver nor the time to go. Nevertheless, the performance of the ZMD–PNG is not inferior to optimal guidance, as will be illustrated in Sec. IV.

One of the main concerns of a guidance engineer interested in implementing the ZMD–PNG law, is its effect on guidance loop stability. Because the guidance loop after linearization is a time-varying system, its stability analysis should be performed with specialized tools, such as the circle criterion. This issue is discussed in Appendix B, where it is shown that stability and ZMD are closely related. Moreover, it is shown in Appendix B that the class of PNG-based systems that remain stable (in the sense of the definition given in Appendix B) until the interception end is a subset of the PNG-based systems yielding ZMD.

The design implication of the preceding discussion may be summarized in the following design principle:

Suppose that the transfer functions $G_1(s)$ and $G_2(s)$ are given. To achieve ZMD, a compensator $K(s)$ should be designed such that $G(s) = K(s)G_1(s)G_2(s)$ is biproper.

The design principle implies that $K(s)$ will necessarily comprise a number of PD controllers. Nevertheless, a considerable performance improvement may be obtained even if the design principle is somewhat loosened, that is, lead–lag compensation is used.

IV. Illustrative Examples

In this section, we consider realistic examples that illustrate the performance of the ZMD–PNG law and compare it to PNG and optimal guidance.

A. Missile Model

The ZMD–PNG design process proposed will be illustrated using a third-order model of $G(s)$. The flight control dynamics are assumed a second-order transfer function with damping ζ and natural frequency ω_n, and the seeker LOS rate measurement dynamics are modeled by a single time lag. As a result, we get

$$G_1(s)G_2(s) = 1 \Big/ \left[(\tau_1 s + 1) \cdot \left(s^2/\omega_n^2 + 2\zeta s/\omega_n + 1\right)\right] \tag{25}$$

Let

$$\tau_1 = 0.3 \text{ s}, \qquad \zeta = 0.5, \qquad \omega_n = 10 \text{ rad/s} \tag{26}$$

Also, assume that

$$N' = 4, \qquad V_C = 1000 \text{ m/s} \tag{27}$$

and that the missile maneuver acceleration is limited by twice the acceleration of the target, that is,

$$\mu_0 \triangleq \frac{\max_t |a_M(t)|}{\max_t |a_T(t)|} = 2 \tag{28}$$

B. ZMD–PNG Design

According to the design principle, we should design a controller $K(s)$ such that $G(s) = K(s)G_1(s)G_2(s)$ is biproper. Consider the following controller:

$$K(s) = \prod_{i=1}^{3} \left(\tau_{Z_i} s + 1\right) \tag{29}$$

Let $\tau_{Z_i} = \tau_Z = 0.23$ s.

Controller (29) shall be called an ideal controller, and the resulting PN-based guidance law will be called ideal ZMD–PNG.

Because $K(s)$ is a PD controller, noise amplification problems might arise. To overcome the problem, the following controller is suggested:

$$K(s) = \prod_{i=1}^{3} \frac{\left(\tau_{Z_i} s + 1\right)}{\left(\tau_{P_i} s + 1\right)} \tag{30}$$

Controller (30) shall be called an actual controller, and the resulting PN-based guidance law will be called actual ZMD–PNG. It is apparent that with this type of a controller, the design principle is not accomplished exactly because the resulting $G(s)$ is not biproper. Nonetheless, if the additional lag is not too large, we can achieve near-ZMD. Thus, let $\tau_{P_i} = \tau_P$ and $\tau_{Z_i} = \tau_Z$. If τ_P is small enough, the phase lag will occur at high frequencies, higher than the typical missile operating frequencies. Thus, no substantial degradation of performance is expected. We chose $\tau_p = 0.05$ s.

The corresponding commanded missile acceleration with the ideal and actual ZMD–PNG are

$$a_C = N' V_C \left[\prod_{i=1}^{3}\left(\tau_{Z_i} s + 1\right)\right]\dot{\lambda}_C, \qquad a_C = N' V_C \left[\prod_{i=1}^{3}\frac{\left(\tau_{Z_i} s + 1\right)}{\left(\tau_{P_i} s + 1\right)}\right]\dot{\lambda}_C$$

C. Optimal Guidance Law

The performance of ZMD–PNG will be compared to optimal guidance. Recall that an optimal guidance law (OGL) for first-order system dynamics and a maneuvering target was first introduced in Ref. 9. It was extensively studied in Refs. 2 and 10. The OGL results from the minimization of the quadratic cost

$$J = \int_0^{t_f} a_c^2(t)\,\mathrm{d}t \tag{31}$$

subject to

$$y(t_f) = 0$$

$$\begin{bmatrix} \dot{y} \\ \ddot{y} \\ \dot{a}_T \\ \dot{a}_M \end{bmatrix} = \begin{bmatrix} 0 & 1 & 0 & 0 \\ 0 & 0 & 1 & -1 \\ 0 & 0 & 0 & 0 \\ 0 & 0 & 0 & -1/\tau_D \end{bmatrix} \cdot \begin{bmatrix} y \\ \dot{y} \\ a_T \\ a_M \end{bmatrix} + \begin{bmatrix} 0 \\ 0 \\ 0 \\ 1/\tau_D \end{bmatrix} a_C \tag{32}$$

where τ_D is the time constant of a first-order system.

The following acceleration command a_c results:

$$a_c = [N'(\theta)/\tau^2]\left[y + \dot{y}\tau + 0.5a_T\tau^2 - a_M\tau_D^2(e^{-\theta} + \theta - 1)\right] \tag{33}$$

where $\theta = \tau/\tau_D$ and

$$N'(\theta) = \frac{6\theta^2(e^{-\theta} + \theta - 1)}{2\theta^3 - 6\theta^2 + 6\theta + 3 - 12\theta e^{-\theta} - 3e^{-2\theta}} \tag{34}$$

Note the following:

1) To implement the OGL, an estimation of time to go and an estimation of target maneuver are required. These tasks, especially the estimation of target maneuver, are not trivial. In the simulations to be presented, we have assumed that the target maneuver is estimated with a delay of 0.2 s, which is quite an optimistic assumption.

2) In most applications, and in our example as well, the system dynamics are of high order, and so there is a mismatch between the system model taken for the OGL design and the actual system model. In this case, τ_D is used to tune the performance of the OGL. We have chosen $\tau_D = 1$ s. One could, of course, try to derive an OGL for the actual system model; however, for high-order systems, this will result in very complicated expressions, whose realization is impractical.

Note that the drawbacks of the OGL do not exist when considering a ZMD–PNG law. Neither the estimation of target maneuver nor time to go is required. Its realization is far simpler, and furthermore, it is not sensitive to uncertainty in system time constant because only the relative order of the dynamics is important.

The performance of the guidance loop is to be evaluated in four cases: PNG, ideal ZMD–PNG, actual ZMD–PNG, and OGL. Also, we consider two types of target maneuvers: a sinusoidal (weave) maneuver and a random telegraph maneuver.

D. Sinusoidal Maneuver

The sinusoidal target maneuver satisfies

$$a_T = a_{T_0}\sin(\omega_T t) \tag{35}$$

Let $a_{T_0} = 1\,g$, $\omega_T = 2.5$ rad/s, and $t_f = 5$ s. We first examine whether ZMD–PNG requires an excessive maneuver effort. Figure 3 shows the absolute value of missile acceleration for the four guidance laws considered. Notice that, in the case of PNG, the acceleration saturates, causing a miss distance of 0.5 m. However, ZMD–PNG

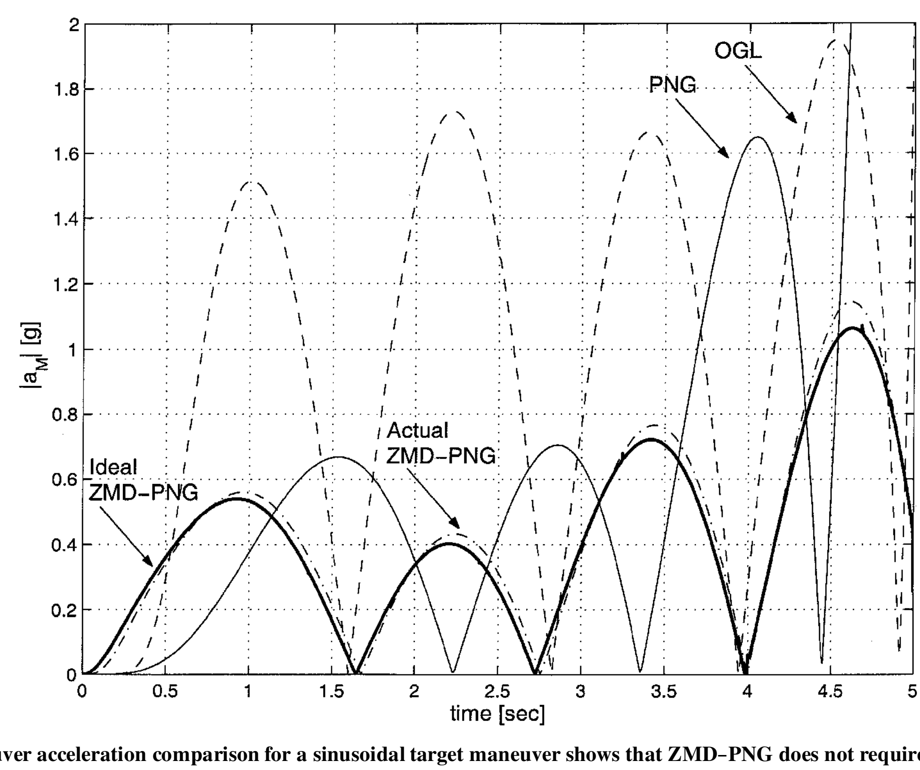

Fig. 3 Missile maneuver acceleration comparison for a sinusoidal target maneuver shows that ZMD–PNG does not require an excessive maneuver effort.

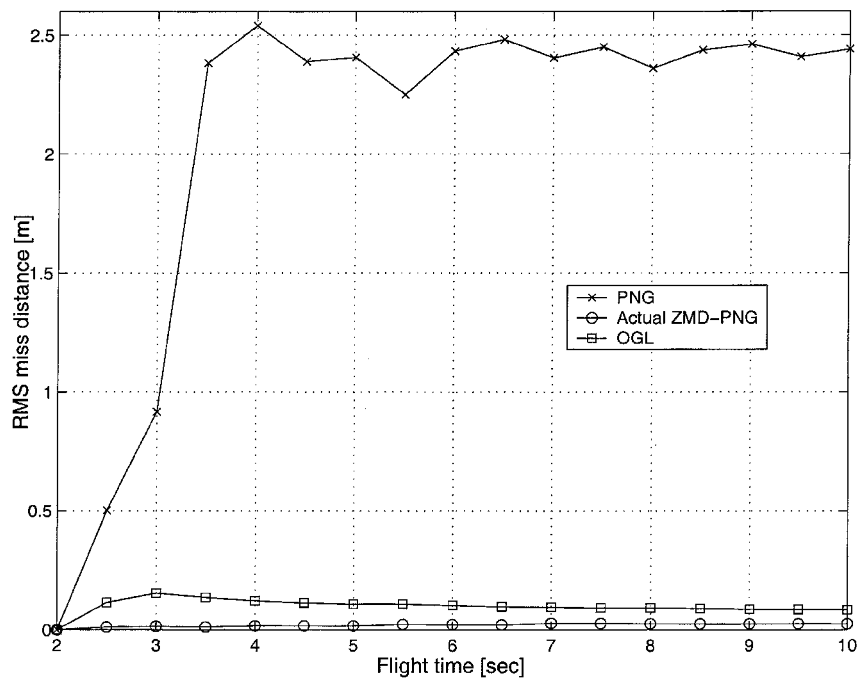

Fig. 4 Comparison of rms miss distances shows that actual ZMD–PNG gives negligible miss distance against a sinusoidal target.

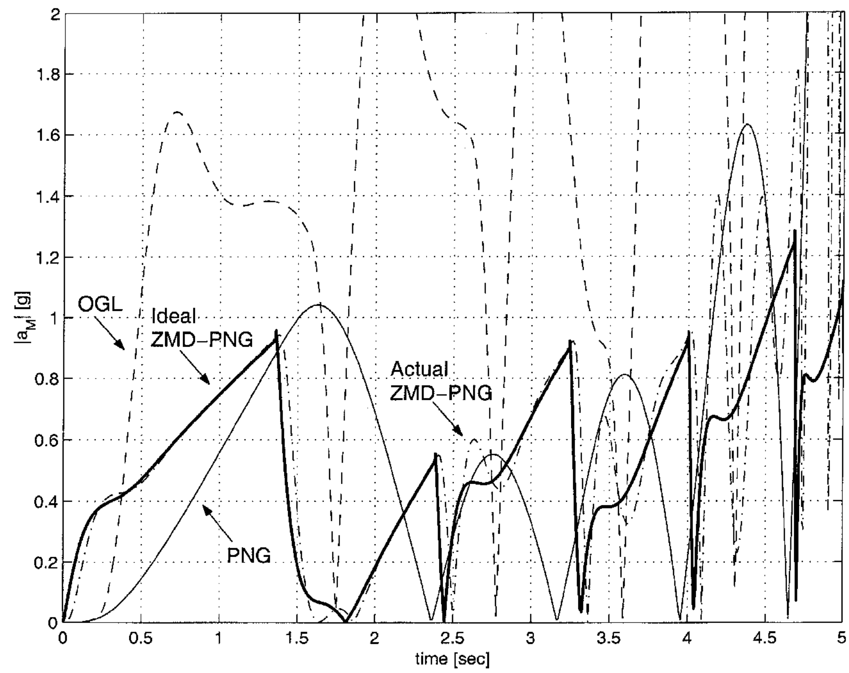

Fig. 5 Maneuver acceleration comparison for a random telegraph target maneuver shows that the acceleration command with ZMD–PNG does not saturate.

does not saturate, either in its ideal or actual form, and the miss distance is negligible. OGL requires a larger maneuver effort than ZMD–PNG. This is because the OGL was designed specifically for first-order systems. When the order of system dynamics is higher, a large maneuver effort is required to compensate the model mismatch.

To examine miss distance, a Monte Carlo simulation was performed. In the Monte Carlo simulation we assumed a sinusoidal target maneuver (35) and the missile model given in Eqs. (25–28). To evaluate the ZMD–PNG performance in a stochastic environment, a zero-mean Gaussian white noise with a standard deviation of 0.05 deg/s was added to the LOS rate measurement. The guidance laws considered were PNG, actual ZMD–PNG, and OGL. Figure 4 shows rms values of miss distance as a function of flight time. It is seen that PNG yields rms miss distances that range from 0.5 to 2.5 m. OGL exhibits a better performance, with an average rms miss of about 0.1 m. Actual ZMD–PNG yields the smallest rms miss distance, of about 0.02 m. The miss distance with actual ZMD–PNG is not identically zero because of the small lag incorporated to deal with noise filtering. Thus, we conclude that the ZMD–PNG considerably improves miss distance, even when the LOS rate measurement is corrupted by noise.

E. Random Telegraph Maneuver

Figure 5 shows the absolute value of missile acceleration for the four guidance laws considered. Some interesting observations can be drawn from Fig. 5. PNG saturates 0.5 s before flight termination. The ideal ZMD–PNG does not saturate. Consequently, it is evident that in the case of a random target maneuver, such as random telegraph, the new guidance law prevents missile acceleration saturation. When a small lag is used, that is, actual ZMD–PNG, the acceleration saturates very close to flight termination, thus causing

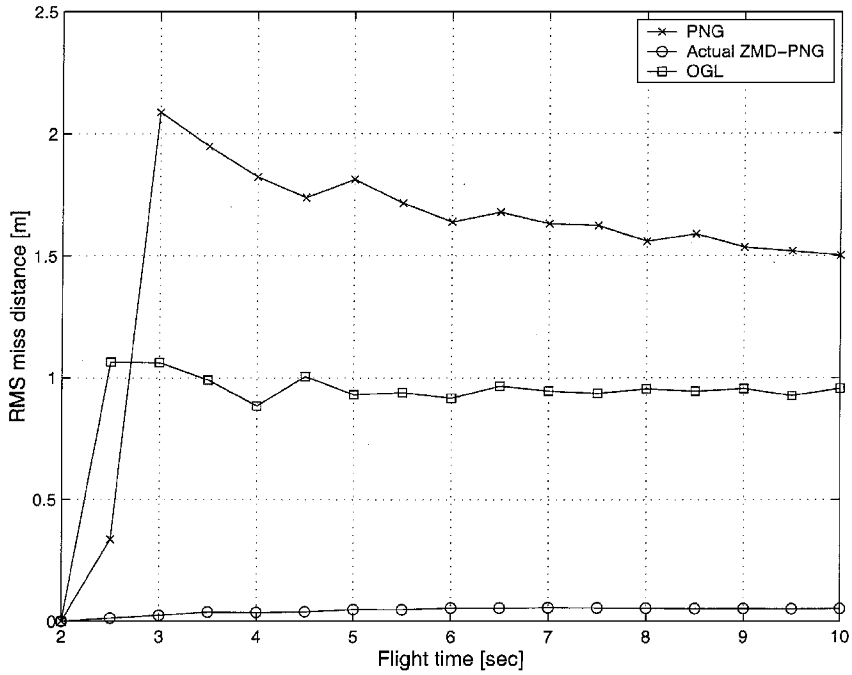

Fig. 6 Comparison of rms miss distances shows that actual ZMD–PNG gives negligible miss distance against a target performing a random telegraph maneuver.

a negligible miss distance. OGL does not exhibit a feasible performance: This guidance law cannot deal adequately with target maneuvers when the missile dynamics are of high order.

A Monte Carlo simulation for the evaluation of miss distance was used in the random telegraph case as well. The guidance laws considered were PNG, actual ZMD–PNG, and OGL. Figure 6 shows rms values of miss distance as a function of flight time. Clearly, PNG yields rms miss distances that range from 1.5 to 2 m. OGL exhibits a better performance, with a miss of about 1 m. Actual ZMD–PNG yields the best performance, with an average rms miss of 0.05 m.

V. Conclusions

In this study, a new guidance law was presented. The derivation of this law comprises of two main stages: First, linear PNG kinematics was adopted. Second, the expressions for miss distance, derived by the method of adjoints, were analyzed. This analysis has shown that ZMD could be obtained for any flight time, provided that the guidance transfer function is biproper. This is true for the following cases: deterministic or random target maneuver and stochastic inputs such as fading and passive- and active-receiver noise.

The design procedure of the new guidance law, ZMD–PNG, involves lead compensation. When the LOS rate measurement is noisy, lead–lag compensation may be used. Simulations of ZMD–PNG that compared its performance to PNG and an OGL have given rise to the following observations:

1) The overall maneuver effort required by the ZMD is smaller than that required by PNG.

2) The miss distance is considerably smaller than that obtained with either PNG or OGL. Actually, it is very close to zero.

Perhaps the main advantage of ZMD–PNG over modern guidance laws is that it does not require the estimation of target maneuver or time to go. It uses LOS rate measurements only.

Finally, note that the best performance of ZMD–PNG is expected in low glint systems, such as missiles with electo-optical seekers. This is due to the inherent lead compensation involved, which makes the system more sensitive to glint effects.

Appendix A: Proof of Theorem

$H(s)$ can be expanded as a series of the following form[21]:

$$H(s) = \sum_{i=1}^{\infty} h_i s^{-i} \tag{A1}$$

The $\{h_i\}$ are known as the Markov parameters of $H(s)$. They are given by

$$[h_1, h_2, \ldots, h_n]^T = T^{-1}(a) \cdot [b_1, b_2, \ldots, b_n]^T \tag{A2}$$

where $T(a)$ is a lower triangular Toeplitz matrix with first column $[1, a_1, \ldots, a_{n-1}]^T$. Note that its inverse always exists. Furthermore, notice that

$$h_1 = b_1 \tag{A3}$$

so that Eq. (A1) can be written as

$$H(s) = \frac{b_1}{s} + \sum_{i=2}^{\infty} h_i s^{-i} \tag{A4}$$

By integrating Eq. (A4), we find that

$$F(x) = b_1 \ln(x) + \sum_{i=2}^{\infty} \frac{h_i}{1-i} x^{1-i} \tag{A5}$$

Thus, $F(\infty) \to 0$ if and only if $b_1 = 0$, that is, $r \geq 2$. Otherwise, for $b_1 > 0$, since $\ln(\infty) \to \infty$, $F(\infty) \to \infty$. □

Note that if $H(s)$ is nonstrictly proper, we can write

$$H(s) = H_p(s) + m(s) \tag{A6}$$

where $H_p(s)$ is strictly proper and $m(s)$ is a polynomial remainder. In this case, $F(\infty) \to \infty$ since

$$\lim_{\sigma \to \infty} \left[\int m(\sigma)\, d\sigma \right] \to \infty$$

Appendix B: Connection Between ZMD–PNG and Loop Stability

It was conjectured in Refs. 12, 13, and 17 that a strong connection exists between system stability and miss distance. In Ref. 13, the concept of FT-GAAS was introduced. When the circle criterion is employed, an analytical expression relating system parameters and the time up to which the PNG system is FT-GAAS was given. Yet, no analytical formulation relating miss distance to FT-GAAS was found. Subsequently, such a relation is proposed. In Ref. 13, the following definition of FT-GAAS was suggested.

Definition B1 (Ref. 13): The linearized PNG system shown in Fig. 2 is FT-GAAS in some time interval $J_{t^*} = [t_0, t^*] \subseteq [t_0, t_f]$ if for some state vector $\boldsymbol{x}(t) \in \Re^n$ there exists $P > 0$ such that $\boldsymbol{x}^T(t)P\boldsymbol{x}(t)$ is a decreasing function of time $\forall x(t_0)$, $\forall t \in J_{t^*}$.

When the circle criterion[22,23] is employed, it is shown[13,16] that FT-GAAS in the interval J_{t^*} is assured provided that the time to go $\tau = t_f - t$ satisfies

$$\tau \geq \tau_0 \triangleq -N' \min_{\omega \neq 0} \mathrm{Re}[H(j\omega)] \tag{B1}$$

where $H(j\omega) = G(j\omega)/j\omega$ is assumed to be minimal and $G(s)$ is assumed to be asymptotically stable with $G(0) = 1$.

We wish to determine the class of transfer functions $H(s)$, for which divergence of the PNG system state variables, in the sense of Definition B1 and Eq. (B1), is avoided. In other words, it is desired to find under what conditions $\tau_0 = 0$. Assume for the moment that such a class exists,

$$\boldsymbol{S} \triangleq \{H(s) : \tau_0 = 0\} \tag{B2}$$

We aim at showing that the class $\boldsymbol{S}$ is a subset of $\boldsymbol{H}$. To do that, we consider the following proposition:

Proposition

$$\boldsymbol{S} \subseteq \boldsymbol{H} \tag{B3}$$

The physical consequence of the proposition is that, if some combination of the state variables of the PNG system (for example, LOS rate, maneuver acceleration, and commanded acceleration) is kept bounded until the end of interception, no miss will occur.

Before proving the proposition, we remind the reader of some facts regarding positive real functions. Denote by (PR) the class of positive-real transfer functions. Next, consider the following definition.

Definition B2 (Ref. 24): A transfer function $H(s)$ is positive real if $\mathrm{Re}[H(s)] \geq 0 \ \ \forall \mathrm{Re}[s] > 0$.

The necessary and sufficient conditions for positive realness are obtained by the following theorem:

Theorem B (Ref. 24): $H(s) \in \{PR\}$ if and only if $H(s)$ is stable, its poles on the imaginary axis are distinct with the associated residues real and nonnegative and, in addition,

$$\mathrm{Re}[H(j\omega)] \geq 0 \quad \forall \omega > 0 \tag{B4}$$

Theorem B and Eq. (B1) lead to the following lemma.

Lemma: Time $\tau_0 = 0$ if and only if $H(s)$ is positive real, that is, $\boldsymbol{S} = \{PR\}$.

Proof: Suppose that $H(s)$ is positive real. Then according to Theorem B, $\mathrm{Re}[H(j\omega)] \geq 0 \ \ \forall \omega > 0$. Because the time to go τ is a nonnegative number, Eq. (B1) gives $\tau_0 = 0$. Now, suppose that $\tau_0 = 0$. If a minimum of a function is zero, it implies that this function is nonnegative; thus, $\mathrm{Re}[H(j\omega)] \geq 0 \ \ \forall \omega > 0$. Also, we assumed that $G(s)$ is asymptotically stable and $G(0) = 1$. Thus, $H(s) = G(s)/s$ is stable, and the residue of $H(s)$ at the distinct pole $s = 0$ is 1. According to Theorem B, these three facts imply that $H(s)$ is positive real. □

Now, we continue with the proof of the proposition. It is well known[24] that for $H(s) \in \boldsymbol{S} = \{PR\}$ it is necessary that

$$r[H(s)] = 0 \qquad \text{or} \qquad 1, b_1 > 0 \tag{B5}$$

Note that Eq. (B5) guarantees that $H(s) \in \boldsymbol{H}$. However, because Eq. (B5) is not a sufficient condition for strictly positive realness, there might be cases in which Eq. (B5) holds, but $H(s) \notin \{PR\}$. Thus, it is true that $\boldsymbol{S} = \{PR\} \subseteq \boldsymbol{H}$, which proves the proposition. □

The preceding discussion underlines that finite time stability in the sense of Definition B1 is strongly associated with miss distance. That is, there is a class of PNG systems for which $\tau_0 = 0$ yields ZMD, but there is a much broader class, the class of biproper (with $b_1 > 0$) transfer functions $G(s)$, which gives ZMD.

References

[1] Shneydor, N., *Missile Guidance and Pursuit*, Horwood, England, U.K., 1998, Chap. 5, pp. 101–124.

[2] Zarchan, P., *Tactical and Strategic Missile Guidance*, Vol. 124, Progress in Astronautics and Aeronautics, AIAA, Washington, DC, 1990, Chaps. 3–5, pp. 37–110.

[3] Rusnak, I., and Meir, L., "Optimal Guidance for High Order and Acceleration Constrained Missile," *Journal of Guidance, Control, and Dynamics*, Vol. 14, No. 3, 1991, pp. 589–596.

[4] Rusnak, I., "Advanced Guidance Laws for Acceleration Constrained Missile, Randomly Maneuvering Target and Noisy Measurement," *Transactions of the IEEE Regional Conference on Aerospace Control Systems*, Inst. of Electrical and Electronics Engineers, New York, 1993, pp. 223–232.

[5] Gutman, S., "On Optimal Guidance for Homing Missiles," *Journal of Guidance, Control, and Dynamics*, Vol. 2, No. 4, 1979, pp. 296–300.

[6] Chang, W. T., and Lin, S. A., "Incremental Maneuver Estimation Model for Target Tracking," *IEEE Transactions on Aerospace and Electronic Systems*, Vol. 28, No. 2, 1992, pp. 439–451.

[7] Hepner, S. A. R., and Geering, H. P., "Adaptive Two-Time-Scale Tracking Filter for Target Acceleration Estimation," *Journal of Guidance, Control, and Dynamics*, Vol. 14, No. 3, 1991, pp. 581–588.

[8] Moose, R. L., "An Adaptive State Estimation Solution to the Maneuvering Target Problem," *IEEE Transactions on Aerospace and Electronic Systems*, Vol. AES-17, No. 3, 1975, pp. 359–362.

[9] Cottrel, R. G., "Optimal Intercept Guidance for Short-Range Tactical Missiles," *AIAA Journal*, Vol. 9, No. 7, 1971, pp. 1414, 1415.

[10] Holder, E. J., and Sylvester, V. B., "An Analysis of Modern Versus Classical Homing Guidance," *IEEE Transactions on Aerospace and Electronic Systems*, Vol. 26, No. 4, 1990, pp. 599–605.

[11] Weiss, H., and Hexner, G., "Modern Guidance Laws with Model Mismatch," *Proceedings of the IFAC Symposium on Missile Guidance*, International Federation of Automatic Control, 1998, pp. 10–21.

[12] Guelman, M., "A Qualitative Study of Proportional Navigation," *IEEE Transactions on Aerospace and Electronic Systems*, Vol. AES-7, No. 4, 1971, pp. 637–643.

[13] Gurfil, P., Jodorkovsky, M., and Guelman, M., "Finite Time Stability Approach to Proportional Navigation Systems Analysis," *Journal of Guidance, Control, and Dynamics*, Vol. 21, No. 6, 1998, pp. 853–861.

[14] Zarchan, P., "Complete Statistical Analysis of Nonlinear Missile Guidance Systems-SLAM," *Journal of Guidance and Control*, Vol. 2, No. 1, 1979, pp. 71–78.

[15] Zarchan, P., "Proportional Navigation and Weaving Targets," *Journal of Guidance, Control, and Dynamics*, Vol. 18, No. 5, 1995, pp. 969–974.

[16] Guelman, M., "The Stability of Proportional Navigation Systems," AIAA Paper 90-3380, July 1990.

[17] Tanaka, T., Hirofumi, E., "Hyperstable Range in Homing Missiles," AIAA Paper 90-3381, July 1990.

[18] Shinar, J., "Divergence Range of Homing Missiles," *Israel Journal of Technology*, Vol. 14, July 1976, pp. 47–55.

[19] Lipman, Y., Shinar, J., and Oshman, Y., "Stochastic Analysis of the Interception of Maneuvering Antisurface Missiles," *Journal of Guidance, Control, and Dynamics*, Vol. 20, No. 4, 1997, pp. 707–714.

[20] Fitzgerald, R. J., "Shaping Filters for Disturbances with Random Starting Times," *Journal of Guidance and Control*, Vol. 2, No. 2, 1979, pp. 152–154.

[21] Kailath, T., *Linear Systems*, Prentice–Hall, Upper Saddle River, NJ, 1980, Chap. 4, pp. 52–70.

[22] Sandberg, I. W., "A Frequency Domain Condition for the Stability of Feedback Systems Containing a Single Time-Varying Nonlinear Element," *Bell System Technical Journal*, Vol. 43, 1964, pp. 1601–1608.

[23] Narendra, K. S., and Goldwyn, R. M., "A Geometrical Criterion for the Stability of Certain Nonlinear Nonautonomous Systems," *IEEE Transactions on Circuit Theory*, Vol. 11, 1964, pp. 406–408.

[24] Slotine, J. J. E., and Li, W., *Applied Nonlinear Control*, Prentice–Hall, Upper Saddle River, NJ, 1991, Chap. 4, pp. 100–144.